AD-A089 720   SRI INTERNATIONAL MENLO PARK CA   F/G 18/3
MISERS BLUFF ELECTROMAGNETIC PROPAGATION EXPERIMENTS. VOLUME II--ETC(U)
OCT 79 J G HAWLEY, A A BURNS   DNA001-77-C-0269
UNCLASSIFIED   DNA-4806T-2   NL

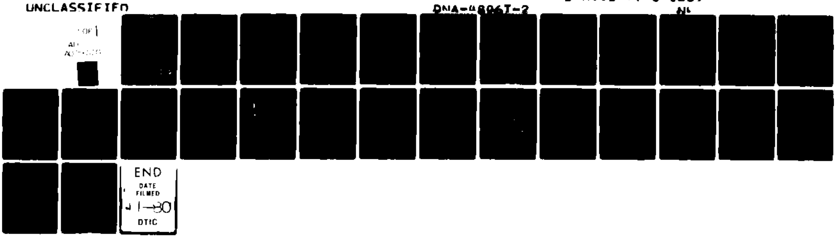

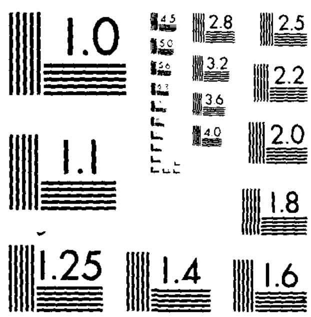

MICROCOPY RESOLUTION TEST CHART
NATIONAL BUREAU OF STANDARDS-1963-A

(12) LEVEL III

DNA 4806T-2

AD A089720

MISERS BLUFF ELECTROMAGNETIC PROPAGATION EXPERIMENTS

Vol II—Preliminary Results of the Laser Experiment

James G. Hawley
Alan A. Burns
SRI International
333 Ravenswood Avenue
Menlo Park, California 94025

1 October 1979

Topical Report for Period 1 October 1978—31 March 1979

CONTRACT Nos. DNA 001-77-C-0269
DNA 001-79-C-0181

APPROVED FOR PUBLIC RELEASE;
DISTRIBUTION UNLIMITED.

THIS WORK SPONSORED BY THE DEFENSE NUCLEAR AGENCY UNDER RDT&E RMSS CODES B322077462 I25AAXHX68501 H2590D, B322078462 I25AAXHX68502 H2590D, AND B322079462 I25AAXHX68503 H2590D.

Prepared for
Director
DEFENSE NUCLEAR AGENCY
Washington, D. C. 20305

Destroy this report when it is no longer needed. Do not return to sender.

PLEASE NOTIFY THE DEFENSE NUCLEAR AGENCY, ATTN: TISI, WASHINGTON, D.C. 20305, IF YOUR ADDRESS IS INCORRECT, IF YOU WISH TO BE DELETED FROM THE DISTRIBUTION LIST, OR IF THE ADDRESSEE IS NO LONGER EMPLOYED BY YOUR ORGANIZATION.

UNCLASSIFIED

SECURITY CLASSIFICATION OF THIS PAGE (When Data Entered)

REPORT DOCUMENTATION PAGE		READ INSTRUCTIONS BEFORE COMPLETING FORM
1. REPORT NUMBER DNA 4806T-2	2. GOVT ACCESSION NO. AD-A084120	3. RECIPIENT'S CATALOG NUMBER
4. TITLE (and Subtitle) MISERS BLUFF ELECTROMAGNETIC PROPAGATION EXPERIMENTS. Volume II. Preliminary Results of the Laser Experiment		5. TYPE OF REPORT & PERIOD COVERED Topical Report for Period 1 Oct 78—31 Mar 79
		6. PERFORMING ORG. REPORT NUMBER SRI Projects 6462 and 8279
7. AUTHOR(s) James G. Hawley, Alan A. Burns		8. CONTRACT OR GRANT NUMBER(s) DNA 001-77-C-0269, DNA 001-79-C-0181
9. PERFORMING ORGANIZATION NAME AND ADDRESS SRI International, 333 Ravenswood Avenue, Menlo Park, California 94025		10. PROGRAM ELEMENT, PROJECT, TASK AREA & WORK UNIT NUMBERS Subtasks I25AAXHX685-01, 02, 03
11. CONTROLLING OFFICE NAME AND ADDRESS Director, Defense Nuclear Agency, Washington, D.C. 20305		12. REPORT DATE 1 October 1979
		13. NUMBER OF PAGES 28
14. MONITORING AGENCY NAME & ADDRESS (if different from Controlling Office)		15. SECURITY CLASS (of this report) UNCLASSIFIED
		15a. DECLASSIFICATION/DOWNGRADING SCHEDULE

16. DISTRIBUTION STATEMENT (of this Report)

Approved for public release; distribution unlimited.

17. DISTRIBUTION STATEMENT (of the abstract entered in Block 20, if different from Report)

18. SUPPLEMENTARY NOTES

This work sponsored by the Defense Nuclear Agency under RDT&E RMSS Codes B322077462 I25AAXHX68501 H2590D, B322078462 I25AAXHX68502 H2590D, and B322079462 I25AAXHX68503 H2590D.

19. KEY WORDS (Continue on reverse side if necessary and identify by block number)

MISERS BLUFF
Nuclear Weapons Effects
Dust and Debris
Electromagnetic Propagation
Laser Systems

20. ABSTRACT (Continue on reverse side if necessary and identify by block number)

A three-wavelength laser radar was fielded at MISERS BLUFF to measure backscatter and extinction values of an explosion-produced dust cloud at wavelengths of 0.532 μm, 1.06 μm, and 10.6 μm. These measurements are important to military designers operating active optical systems in such an environment, and for the understanding of cloud dynamics.

Good-quality backscatter data at the three wavelengths were obtained to T + 30 min on both events. Better-quality transmission data were taken on

DD FORM 1 JAN 73 1473 EDITION OF 1 NOV 65 IS OBSOLETE

UNCLASSIFIED

SECURITY CLASSIFICATION OF THIS PAGE (When Data Entered)

20. ABSTRACT (Continued) micrometers

the second event. At early times, the attenuation in the MBII-2 cloud was greater than 144 dB for the 1.06-μm wavelength, and 124 dB and 70dB for the 0.532-μm and 10.6-μm wavelengths, respectively.

Further analysis will be required to assess the backscatter extinction for the three wavelengths. Comparisons will be made with millimeter-wave radar results and in-situ particle-sampling data.

PREFACE

The material comprising this topical report is virtually the same as that to be published in the proceedings of the MISERS BLUFF Data Review Meeting, held in Albuquerque, NM, in March 1979. Because of the interest in our measurements, we have decided to publish these preliminary results as a separate entity.

TABLE OF CONTENTS

LIST OF ILLUSTRATIONS

LIST OF TABLES

I INTRODUCTION

During Project MISERS BLUFF, SRI International fielded a three-wavelength autotracking lidar to measure the volume backscatter and the extinction coefficients of the explosion-produced dust cloud. These data are relevant to two fields: cloud development, and the operation of active optical systems in the battlefield environment.

This was one of four experiments fielded by SRI International for MISERS BLUFF. The others are described and discussed in separate reports.[1,2*]

Both MISERS BLUFF II tests took place at the Planet Ranch test site on the dry bed of the Bill Williams River near Lake Havasu City, Arizona. The first test, MISERS BLUFF II-1 (MBII-1), which was a 120-ton ammonium nitrate and fuel oil (ANFO) detonation, took place at 1300 MST on 28 June 1978. The second test, MBII-2, consisted of the simultaneous detonation of six such 120-ton ANFO charges uniformly spaced on the periphery of a 100-m-radius circle. This test took place at 1100 MST on 30 August 1978. Although the primary objective of the MBII tests was the study of ground motions in a multiple-burst environment in support of the MX program, the tests provided a good opportunity to measure dust effects as well. Our experiments were added and were conducted on a noninterference basis.

Three lidar wavelengths (see Figure 1) were used to assess the effect of cloud-particle size distributions on the extinction and scattering properties of the cloud. In addition, the laser results will be compared with the millimeter-wave radar results to provide cloud-particle size information as a function of time and cloud morphology. The lidar and radar experiments are in many ways complementary.

---

*All references are listed at the end of the report.

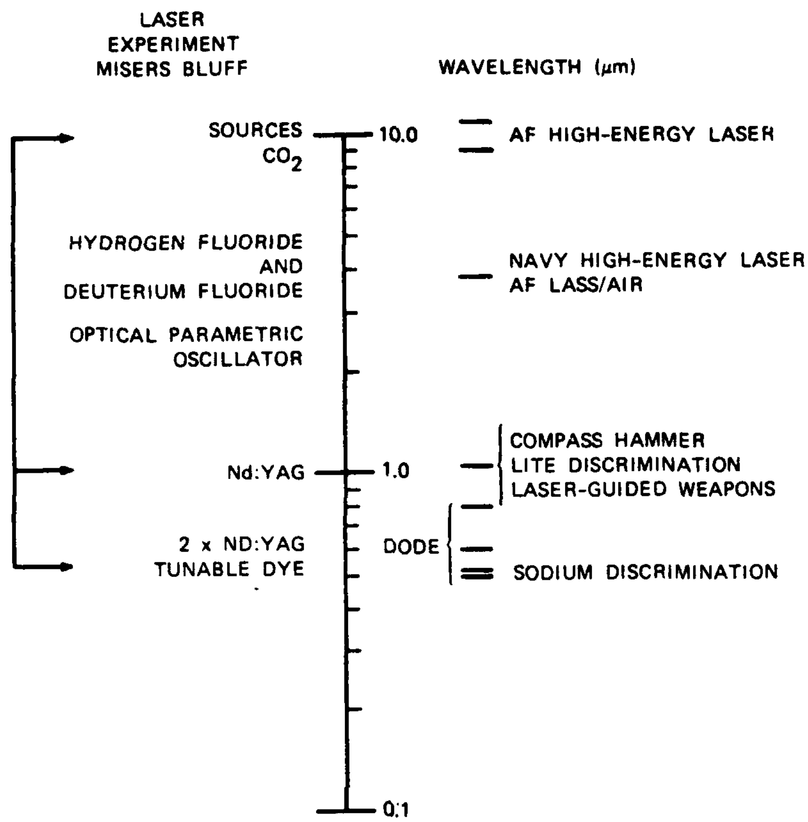

FIGURE 1 OPTICAL WAVELENGTHS RELEVANT TO PROJECT MISERS BLUFF

The other important objective of the laser experiment is the provision of experimental information useful to designers of military systems incorporating designators, rangefinders, and high-energy lasers. The 1.06-μm wavelength from the Nd:YAG laser is now becoming the most widespread designator source in the military inventory. The other designator/rangefinder wavelengths are 0.9 μm and 0.7 μm--emanating from the GaAs and ruby lasers. The 0.532-μm wavelength in the SRI experiment was generated by frequency-doubling the output of the Nd:YAG. This bracketed the wavelengths covering the wavelengths of the designator/rangefinder and the peak of the human-eye response (0.55 μm). The appropriate military systems operating at these wavelengths are LITE, COMPASS HAMMER, sodium discrimination, and the DODE optical intelligence system.

The 10.6 μm laser experiment at MISERS BLUFF was important because it extends the wavelength region spanned from 1.06 μm to 10.6 μm. Most notable of the systems using this range of wavelength are the Air Force HEL system (CO_2 laser at 10.6 μm), and the Air Force and Navy DF laser systems at 3.8 μm.

It was expected that a 10.6-μm laser would penetrate the cloud better than the shorter wavelengths. The higher density of smaller particles should favor transmission of the longer wavelengths, including millimeter-wave radars. Because of the soil characteristics, the MISERS BLUFF dust clouds may have had an unusually large proportion of small particles.

II EXPERIMENT

In order to study the cloud for backscatter and extinction, the following requirements must be met:

(1) Adequate sensitivity at three wavelengths

(2) Collinear beams

(3) Scan capability
Elevation axis = 45°
Azimuth azis = 180°

(4) Collocated receivers for all three wavelengths

(5) Flyable and fixed retroreflector arrays.

The experimental approach requires that both extinction and backscatter be measured simultaneously. For example, the lidar equation (a variant of the well-known radar equation) is

$$P_r(R) = P_t \frac{A_r\left(\frac{c\tau}{2}\right) \beta_\pi (R)\left(\exp -2\int_0^r \alpha(r)dr\right)}{R^2} + P_{BKG}$$

where P_r, P_t = Received and transmitted output powers

A_r = Receiver area

R = Range from the lidar

$(c\tau/2)$ = Laser pulse spatial extent, with τ = laser pulse width, and c = speed of light

$\beta_\pi (R)$ = Volume backscatter coefficient

$\alpha(r)$ = Extinction coefficient

P_{BKG} = Power due to background.

Extinction was measured by monitoring the echoes from a retroreflector array located on Black Mesa, 1.4 km beyond ground zero away from the lasers. After the wind moved the cloud transversely and uncovered the

array, the helicopter-borne retroreflector was directed behind the cloud. The helicopter, moving under ground control instructions, was directed to cover as much of the cloud as possible. It was expected that tracking the helicopter array manually would be extremely difficult. Therefore, an autotracker system was built as an adjunct to the lidar.

The system block diagram is given in Figure 2. The system is housed in a 40-ft-long van. The lidar optics, consisting of the laser and the twin telescope receivers, stand on a framework extending down through the floor of the van and resting on the ground. The optical system filled the back two-thirds of the van. The autotracker and the electronics for the data transmission to the radar van, occupied the front third.

The laser system consisted of a pulsed Nd:YAG laser and a high-power pulsed Transverse-Electrical-Atmospheric (TEA) CO_2 laser. The 1.06-μm output of the Nd:YAG laser was frequency doubled to 0.532 μm using a KD*P-Type-II doubler (see Table 1). The remaining 1.06-μm radiation was transmitted collinearly and in synchronism with the 0.532 μm radiation. The third wavelength, at 10.6 μm, was brought together with the former two beams, by using a special mirror with a central hole. That is, the 1.06/0.532-μm radiation was introduced through a 15-mm hole in the back while the 10.6-μm radiation was reflected from the front surface at 45°. The 10.6-μm radiation emanates from an unstable resonator laser cavity so that in the near field there is no energy in the central region. The hole-in-mirror technique allowed an elegant solution in constructing a three-wavelength laser experiment using widely varying wavelengths.

The three wavelengths were directed out of the van and collinearly with receiver field-of-view by using a series of mirrors in the Coudé configuration. The receivers consisted of a 16-inch-diameter Schmidt-Cassegrain telescope mounted in the az/el configuration and a 12-inch Newtonian mounted alongside. The 16-inch telescope was used for collection of the 1.06/0.532-μm radiation, while the Newtonian telescope was used for collection of 10.6-μm radiation. The detector package for the 1.06/0.532-μm radiation was situated at the Cassegrain focus. A dichroic

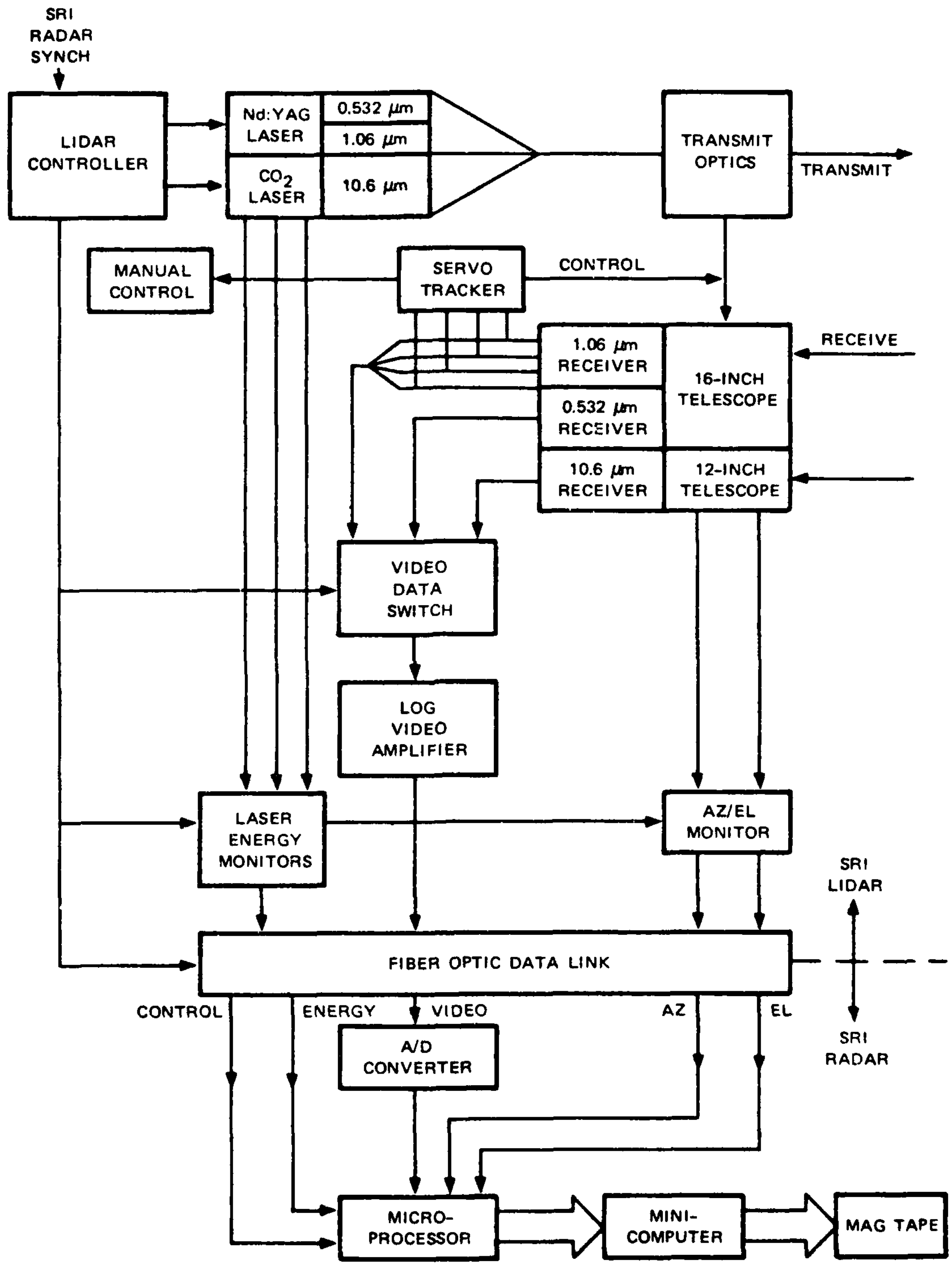

FIGURE 2 LASER EXPERIMENT SYSTEM BLOCK DIAGRAM

Table 1

LASER PARAMETERS

	Nd:YAG Laser		CO_2 Laser
Wavelength	1.06 μm	0.532 μm	10.6 μm (Multiline)
Energy per pulse	150 mJ	50 mJ	1-2 J (MBII-1) 0.3 J (MBII-2)
Pulsewidth	10 ns	8 ns	200 ns (MBII-1) 75 ns (MBII-2)
PRF	10 Hz	10 Hz	0.25 Hz (MBII-1) 1 Hz (MBII-2)
Divergence (10 dB below peak)	1 mrad	1 mrad	1.2 mrad

beam splitter directed the received beams to the appropriate detectors. The receiver parameters are given in Table 2.

The autotracking system was constructed to enable the lidar to follow the helicopter-borne retroreflector at long ranges behind the cloud when manual tracking could not be done. The standard monopulse-radar technique was used. Error signals to the tracking motors were generated by the 1.06-μm 4-quadrant receiver. A narrow gate provided range tracking. A boresighted TV camera with a telephoto lens filtered for viewing at 1.06 μm, enabled manual tracking.

The stationary retroreflector array consisted of 12 front-surface-mirror corner cubes each 5 inches in diameter. When the 1.06-μm experiment was added to the overall laser experiment, an all-reflective array was required rather than a Scotchlite target, which uses the refractive properties of plastics to retroreflect light. The helicopter-borne reflector consisted of 12 retroreflectors spaced equally distant from each other on the surface sphere (icosahedral arrangement). The motion of the array, which hung free beneath the helicopter, allowed the returns from the retroreflectors to be averaged.

Table 2

RECEIVER PARAMETERS

	Wavelength 1.06 μm	Wavelength 0.532 μm	Wavelength 10.6 μm
Telescope	16-inch Schmidt-Cassegrain 176-inch focal length	16-inch Schmidt-Cassegrain 176-inch focal length	12-inch Newtonian 36-inch focal length
Detector	Silicon pin diode, quadrant array with integral preamps	Photomultiplier Gain = 10^4 S-20 response	Hg-Cd-Te $D^* = 1.1 \times 10^{10}$ cm $Hz^{1/2}/W$ 1 mm diameter
Filter	5.0 nm at 1.064 nm T = 65%	0.23 nm at 0.5323 nm T = 30%	None
Field of view	1.9 mrad	1.9 mrad	3.0 mrad

Data from the receivers were fed through a video log amplifier and then fed (via optical-fiber data links) to the SRI radar van for digitization and storage on tape. A microprocessor handled the interlacing of lidar data, with radar data, so that the same A/D converter could be used for both. Housekeeping data, such as azimuth, elevation, laser energy, which laser data was being recorded, and certain status bits were transmitted over parallel fiber-optic data links. The 1.06-μm and 0.532-μm returns were recorded, alternatively, each 100 ms, and the 10.6-μm return was inserted into the data stream each second.

III EXPERIMENTAL RESULTS

The SRI laser experiment was fielded at the Planet Range site, two weeks before MBII-1. The experiment was readied in the remaining time. Many tests were performed with the helicopter-borne retroreflector, to optimize the tracker. The tracker seemed to work well, locking onto stationary targets such as the retroreflector array atop Black Mesa, but did not maintain lock while tracking the helicopter.

Because of high winds at event time, the MBII-1 cloud did not occult the retroreflector array; therefore, we immediately began to manually scan the cloud. All wavelengths (0.532 μm, 1.06 μm, and 10.6 μm) were operational. Figure 3 gives range-time intensity plots (RTI) of the received echoes from the cloud for the 0.532-μm wavelength for the first 11 minutes after detonation. The main cloud was optically thick but there were other, thinner clouds situated about 0.75 km in front of the main cloud. These are probably caused by ground shocks ejecting dust far from the main event. These same clouds, rising from the desert floor, can be observed on photographs.

The MBII-1 cloud was scanned for about 20 min, while we attempted to acquire the helicopter track. This was very difficult, so only one track was undertaken--at about T + 25 min. Because of the high winds aloft ($\approx$35 knots), the cloud quickly moved beyond the 16-km maximum range of the laser experiment.

Just before MBII-2, the field team again set up the laser experiment--this time concentrating on calibrations and beam-pattern measurements. More tracking work was undertaken with the helicopter-borne retroreflector, but the results were disappointing. The helicopter-borne array was designed to exhibit at least one corner cube at all angles; however, at longer ranges, the waiting time between consecutive echoes caused the autotracker to hunt and then totally lose track. That is, the combination of the intensity of the return and the sampling interval was inadequate

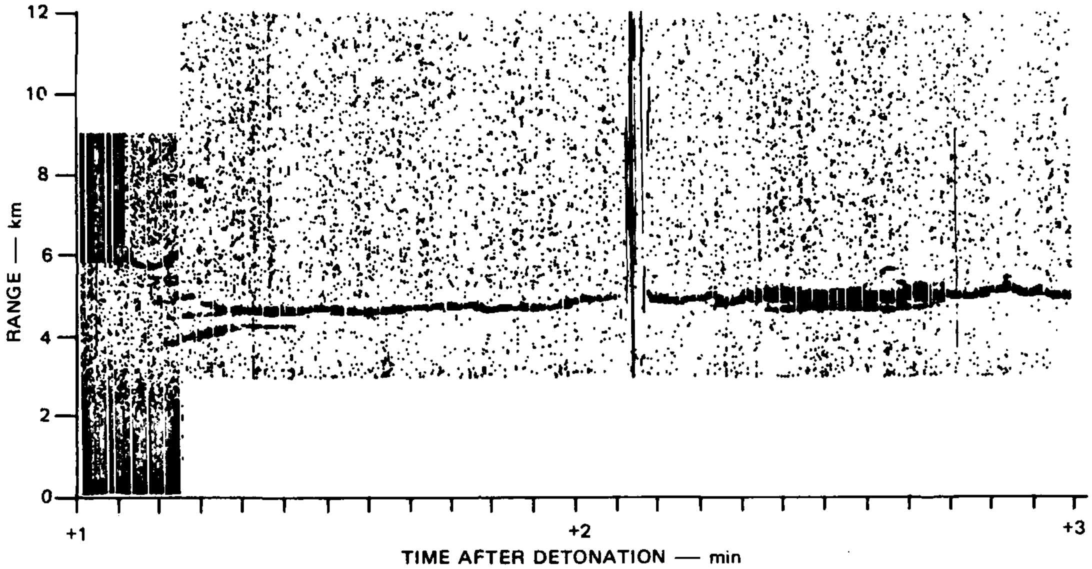

(a) T + 1 min THROUGH T + 3 min

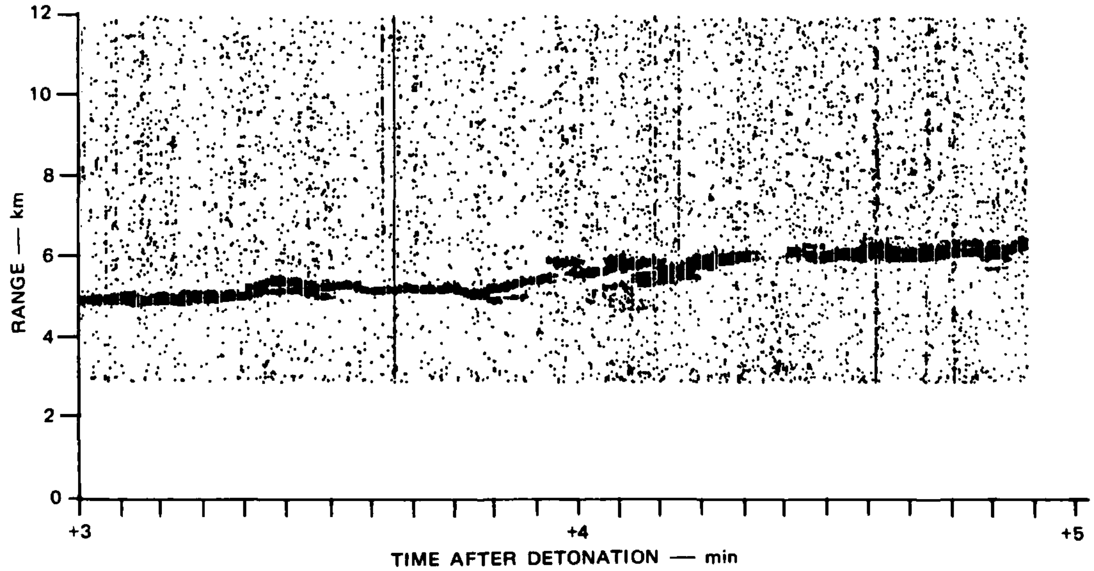

(b) T + 3 min THROUGH T + 5 min

FIGURE 3 MBII-1 LIDAR DATA AT 0.53 μm, INTENSITY AS A FUNCTION OF RANGE AND TIME

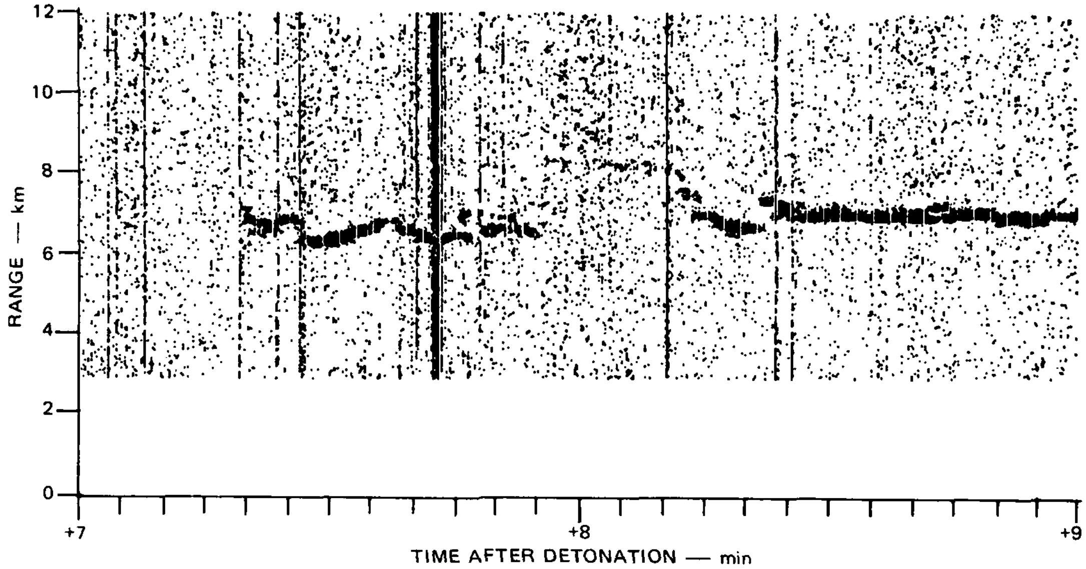

(c) T + 7 min THROUGH T + 9 min

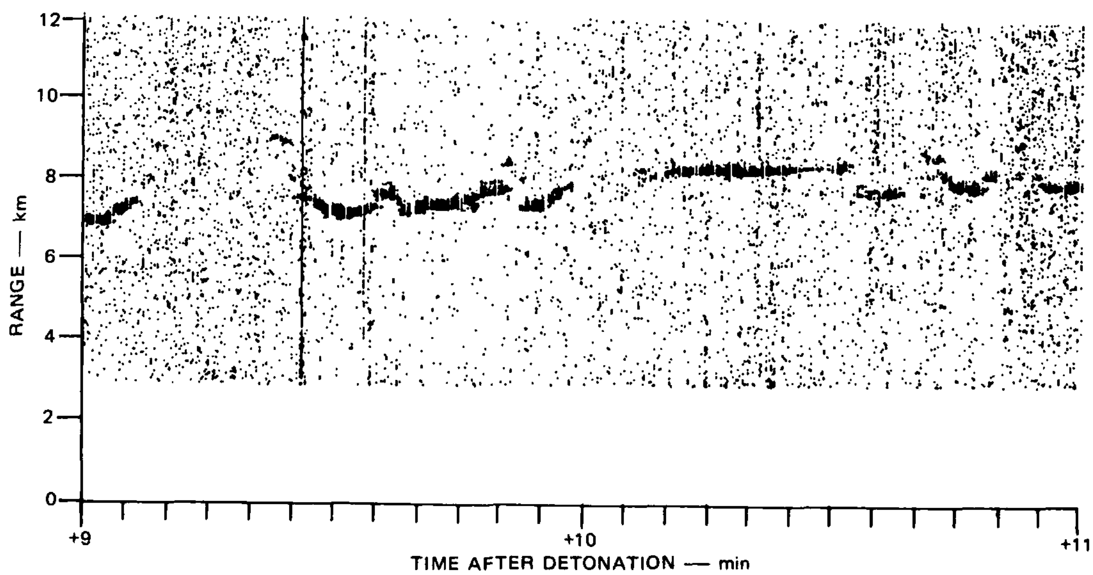

(d) T + 9 min THROUGH T + 11 min

FIGURE 3 (Concluded)

to allow consistent tracking. Only one or two of the twelve retroreflectors were illuminated by the lasers at any one time.

The MBII-2 dust cloud rose and occulted the fixed retroreflector array for 3 min. At T + 2 min, the lasers were still pointed at the fixed array--at the stem of the dust cloud. At T + 3 min, the stem, which was moving to the northwest, uncovered the array. Figures 4 and 5 show the preliminary RTI plot for all wavelengths from T - 0 to T + 4 min.

Apparently, all three wavelength echoes from the retroreflector array came back into view at approximately the same time. (However, there may have been a data recording problem at 10.6 μm.) Further data analysis, using the appropriate calibrations, is needed to determine the ability of the three wavelengths to penetrate the cloud at around T + 3 min.

During the occultation period, only the minimum attenuation can be deduced. Preshot measurements of the signal return of the retroreflector echoes had to be attenuated enough to fall in the linear region of the detector system. The maximum values of signal-to-noise ratio that the SRI laser experiment could accommodate from a two-way retroreflected laser pulse through the MBII-2 cloud at early times are as follows:

Wavelength	SNR
0.532 μm	124 dB
1.06 μm	104 dB
10.6 μm	70 dB

During the period T + 4 min to T + 6 min, the cloud was scanned manually while the helicopter pilot was instructed to fly out from a hover position over the Planet Ranch air strip. This strategy, while taking a little longer, assured acquisition of the helicopter track from the start. The helicopter was tracked from T + 8 min to T + 15 min. Most tracking was done manually. Figure 6 shows the echoes from the helicopter when it was positioned behind the cloud, for transmission measurements at the three wavelengths. A second helicopter track was undertaken at T + 35 min. In both cases, track was broken when the operator

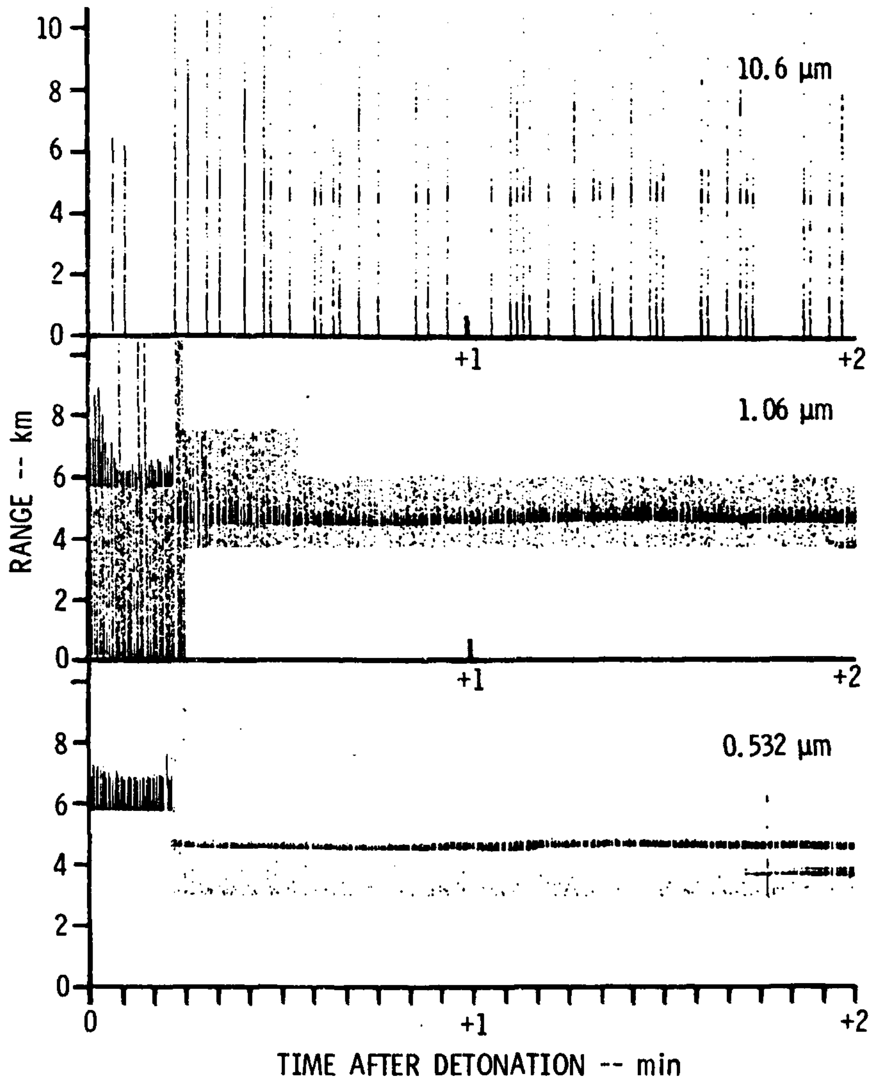

FIGURE 4 MBII-2 LIDAR DATA, INTENSITY AS A FUNCTION OF RANGE AND TIME, T_0 THROUGH T + 2 min

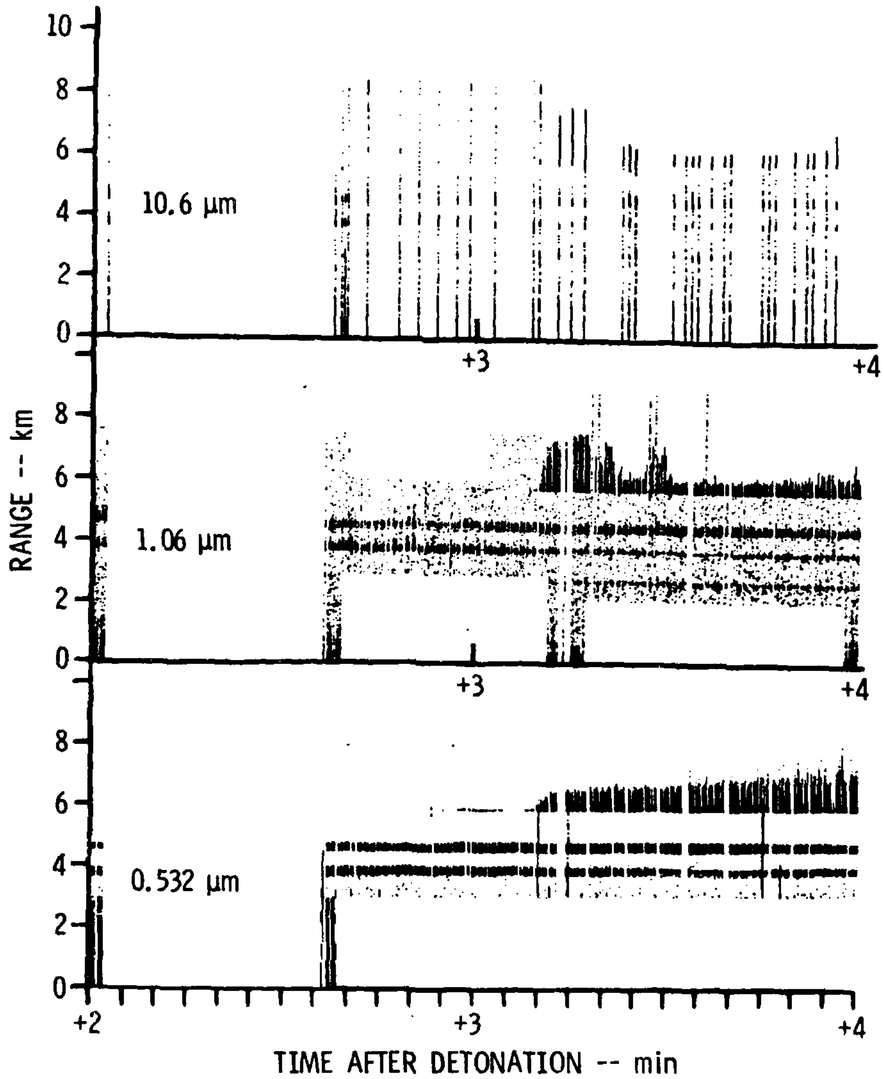

FIGURE 5 MBII-2 LIDAR DATA, INTENSITY AS A FUNCTION OF RANGE AND TIME, T + 2 min THROUGH T + 4 min

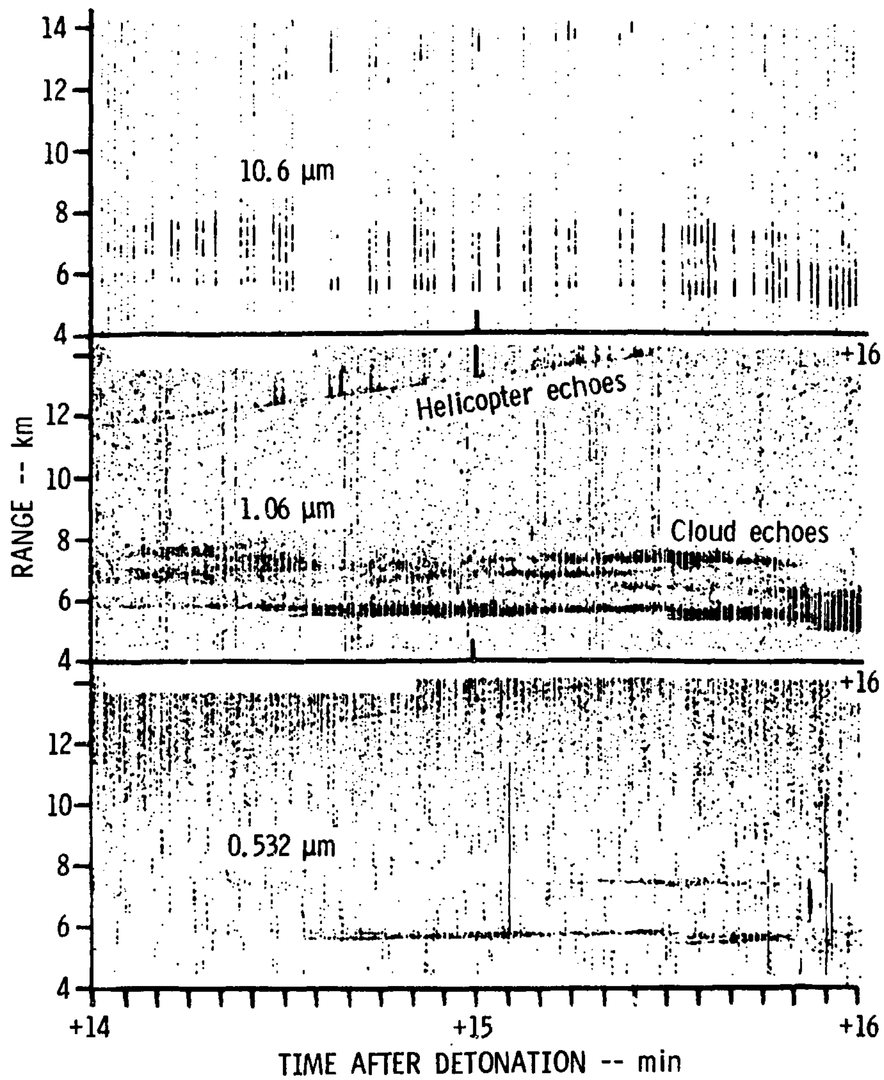

FIGURE 6 MBII-2 LIDAR DATA, INTENSITY AS A FUNCTION OF RANGE AND TIME, T + 14 min THROUGH T + 16 min

viewing the helicopter in the TV screen could no longer see it because of the cloud. Backscatter from the cloud was still quite strong.

IV CONCLUSIONS

The results so far show that the optical attenuation for the MBII-2 event at early times was deeper than 104 dB for the 1.06-μm wavelength, and 124 dB and 70 dB for the 0.532-μm and 10.6-μm wavelengths, respectively. Optically thin clouds situated from hundreds of meters to several kilometers from the main event were associated with the event and were probably caused by shock waves. Further processing of the laser data to correct for system response will have to be performed to assess the meaning of the data across all three wavelengths.

A mathematical technique is being investigated to estimate the volume backscatter coefficient when the extinction coefficient is known. It is expected that an iterative technique will be applied to the coefficients so that they converge to physically realizable values. A comparison of the coefficients at the three wavelengths will be compared with in-situ particle-size data, as well as millimeter-wave radar data where appropriate.

REFERENCES

1. A. A. Burns, "MISERS BLUFF Electromagnetic Propagation Experiments: Preliminary Results of the UHF-EHF-Radar-Scattering and Coherent-Transmission Experiments," Topical Report for the Period 10 October 1978 to 31 March 1979, Contracts DNA001-77-C-0269 and DNA001-79-C-0181, SRI Projects 6462 and 8279, SRI International, Menlo Park, CA, 94025 (unpublished).

2. R. S. Vickers, "Medium Frequency Propagation at MISERS BLUFF," Topical Report for the Period 15 July to 15 November 1978, Contract DNA001-77-C-0269, SRI Project 6462, SRI International, Menlo Park, CA, 94025 (unpublished).

DISTRIBUTION LIST

DEPARTMENT OF DEFENSE

Assistant Secretary of Defense
Comm., Cmd., Cont. & Intell.
ATTN: C3IST&CCS, M. Epstein
ATTN: Dir. of Intelligence Systems, J. Babcock

Assistant to the Secretary of Defense
Atomic Energy
ATTN: Executive Assistant

Defense Advanced Rsch. Proj. Agency
ATTN: TIO

Defense Communications Agency
ATTN: Code 101B
ATTN: Code 205
ATTN: Code 480, F. Dieter

Defense Communications Engineer Center
ATTN: Code R410, R. Craighill
ATTN: Code R123

Defense Nuclear Agency
3 cy ATTN: RAAE
4 cy ATTN: TITL

Defense Technical Information Center
12 cy ATTN: DD

Field Command
Defense Nuclear Agency
ATTN: FCPR

Field Command
Defense Nuclear Agency
Livermore Division
ATTN: FCPRL

Interservice Nuclear Weapons School
ATTN: TTV

Joint Chiefs of Staff
ATTN: C3S Evaluation Office

Undersecretary of Defense for Rsch. & Engrg.
ATTN: Strategic & Space Systems (OS)

WWMCCS System Engineering Org.
ATTN: R. Crawford

DEPARTMENT OF THE ARMY

Atmospheric Sciences Laboratory
U.S. Army Electronics R&D Command
ATTN: DELAS-EO, F. Niles

BMD Advanced Technology Center
Department of the Army
ATTN: ATC-T, M. Capps
ATTN: ATC-R, D. Russ
ATTN: ATC-O, W. Davies

BMD Systems Command
Department of the Army
ATTN: BMDSC-HW

DEPARTMENT OF THE ARMY (Continued)

Harry Diamond Laboratories
Department of the Army
ATTN: DELHD-N-P
ATTN: DELHD-N-P, F. Wimenitz
ATTN: DELHD-I-TL, M. Weiner

U.S. Army Materiel Dev. & Readiness Cmd.
ATTN: DRCLDC, J. Bender

U.S. Army Missile Intelligence Agency
ATTN: J. Gamble

U.S. Army Nuclear & Chemical Agency
ATTN: Library

U.S. Army Satellite Comm. Agency
ATTN: Document Control

U.S. Army TRADOC Systems Analysis Activity
ATTN: ATAA-PL

DEPARTMENT OF THE NAVY

Naval Electronic Systems Command
ATTN: PME 117-20
ATTN: Code 501A
ATTN: PME 117-211, B. Kruger
ATTN: PME 117-2013, G. Burnhart

Naval Research Laboratory
ATTN: Code 4780, S. Ossakow
ATTN: Code 4700, T. Coffey

Naval Surface Weapons Center
ATTN: Code F31

Office of Naval Research
ATTN: Code 465

Strategic Systems Project Office
Department of the Navy
ATTN: NSP-43
ATTN: NSP-2722, F. Wimberly

DEPARTMENT OF THE AIR FORCE

Air Force Geophysics Laboratory
ATTN: OPR, A. Stair
ATTN: OPR, H. Gardiner
ATTN: PHI, J. Buchau
ATTN: PHP, J. Mullen

Air Force Weapons Laboratory
Air Force Systems Command
ATTN: DYC
ATTN: SUL

Air Force Wright Aeronautical Laboratories
ATTN: AAD, W. Hunt
ATTN: A. Johnson

Ballistic Missile Office
Air Force Systems Command
ATTN: MNNH, M. Baran

DEPARTMENT OF THE AIR FORCE (Continued)

Deputy Chief of Staff
Research, Development, & Acq.
Department of the Air Force
ATTN: AFRDQ

Headquarters Space Division
Air Force Systems Command
ATTN: SKA, M. Clavin

Headquarters Space Division
Air Force Systems Command
ATTN: SZJ, W. Mercer
ATTN: SZJ

Strategic Air Command
Department of the Air Force
ATTN: XPFS
ATTN: NRT

DEPARTMENT OF ENERGY CONTRACTORS

EG&G, Inc.
Los Alamos Division
ATTN: D. Wright
ATTN: J. Colvin

Lawrence Livermore Laboratory
ATTN: L-31, R. Hager
ATTN: L-389, R. Ott

Los Alamos Scientific Laboratory
ATTN: E. Jones
ATTN: D. Simons
ATTN: MS 664, J. Zinn

Sandia Laboratories
ATTN: Org. 1250, W. Brown
ATTN: Org. 4241, T. Wright

OTHER GOVERNMENT AGENCY

Institute for Telecommunications Sciences
National Telecommunications & Info. Admin.
ATTN: W. Utlaut

DEPARTMENT OF DEFENSE CONTRACTORS

Aerospace Corp.
ATTN: D. Olsen
ATTN: N. Stockwell
ATTN: V. Josephson

Berkeley Research Associates, Inc.
ATTN: J. Workman

Charles Stark Draper Lab., Inc.
ATTN: D. Cox
ATTN: J. Gilmore

ESL, Inc.
ATTN: J. Marshall

General Electric Co.
ATTN: A. Harcar
ATTN: M. Bortner

General Research Corp.
ATTN: J. Ise, Jr.
ATTN: J. Garbarino

DEPARTMENT OF DEFENSE CONTRACTORS (Continued)

General Electric Company-TEMPO
ATTN: W. McNamara
ATTN: W. Knapp
ATTN: M. Stanton
ATTN: T. Stevens
ATTN: DASIAC

Georgia Institute of Technology
ATTN: E. Martin

GTE Sylvania, Inc.
ATTN: M. Cross

HSS, Inc.
ATTN: D. Hansen

Institute for Defense Analyses
ATTN: E. Bauer

JAYCOR
ATTN: S. Goldman

Johns Hopkins University
ATTN: T. Potemra

Kaman Sciences Corp.
ATTN: T. Meagher

Lockheed Missiles & Space Co., Inc.
ATTN: D. Churchill

M.I.T. Lincoln Lab.
ATTN: D. Towle

Martin Marietta Corp.
ATTN: R. Heffner

McDonnell Douglas Corp.
ATTN: R. Halprin
ATTN: W. Olson
ATTN: G. Mroz

Meteor Communications Consultants
ATTN: R. Leader

Mission Research Corp.
ATTN: R. Hendrick
ATTN: R. Kilb
ATTN: D. Sappenfield
ATTN: S. Gutsche
ATTN: F. Fajen
ATTN: D. Sowle
ATTN: R. Bogusch

Mitre Corp.
ATTN: B. Adams

Mitre Corp.
ATTN: W. Hall
ATTN: W. Foster
ATTN: J. Wheeler

Photometrics, Inc.
ATTN: I. Kofsky

Physical Dynamics, Inc.
ATTN: E. Fremouw

DEPARTMENT OF DEFENSE CONTRACTORS (Continued)

R & D Associates
ATTN: W. Karzas
ATTN: R. Lelevier
ATTN: B. Gabbard
ATTN: C. MacDonald
ATTN: F. Gilmore

R & D Associates
ATTN: B. Yoon

Rand Corp.
ATTN: C. Crain
ATTN: E. Bedrozian

Science Applications, Inc.
ATTN: D. Hamlin
ATTN: J. McDougall
ATTN: L. Linson
ATTN: D. Sachs

Science Applications, Inc.
ATTN: D. Divis

DEPARTMENT OF DEFENSE CONTRACTORS (Continued)

Science Applications, Inc.
ATTN: J. Cockayne

SRI International
ATTN: W. Jaye
ATTN: G. Smith
ATTN: W. Chesnut
ATTN: R. Leadabrand
ATTN: C. Rino
ATTN: M. Baron

Technology International Corp.
ATTN: W. Boquist

Teledyne Brown Engineering
ATTN: R. Deliberis

TRW Defense & Space Sys. Group
ATTN: R. Plebuch

Visidyne, Inc.
ATTN: J. Carpenter
ATTN: C. Humphrey

LME